IET Communications

Research Article

IET Journals
The Institution of Engineering and Technology

Throughput enhancement of IEEE 802.11ad through space-time division multiple access scheduling of multiple co-channel networks

ISSN 1751-8628
Received on 23rd February 2015
Revised on 25th October 2015
Accepted on 14th November 2015
doi: 10.1049/iet-com.2015.0184
www.ietdl.org

Wei Feng[1], Yong Niu[1], Yong Li[1] ✉, Bo Gao[1], Li Su[1], Depeng Jin[1], Dapeng Oliver Wu[2]

[1]Department of Electronic Engineering, State Key Laboratory on Microwave and Digital Communications, Tsinghua National Laboratory for Information Science and Technology (TNLIST), Tsinghua University, Beijing 100084, People's Republic of China
[2]Department of Electrical and Computer Engineering, University of Florida, Gainesville, FL 32611-6130, USA
✉ *E-mail: liyong07@tsinghua.edu.cn*

Abstract: 60-GHz millimetre-wave (mm-wave) communication is gradually becoming a promising candidate for the next generation wireless system to meet the demands of mobile applications. To compensate for high path loss, directional links are established in mm-wave communication system, which adds opportunity for spatial reuse. As one of its most promising protocols for commercial production, IEEE 802.11ad standard provides a mechanism to support space-time division multiple access (STDMA) within a single network. However, the interference level among different co-channel networks is much lower than that inside a network, which provides greater potential for spatial reuse. In this study, based on the architecture and timing structure of IEEE 802.11ad, the authors propose a spatial reuse strategy among multiple co-channel networks. They formulate the problem as a mixed-integer non-linear programming problem, and then propose an inter-network STDMA scheduling algorithm, which considers clustering frame structure in IEEE 802.11ad, and combines greedy principle and mutual interference avoidance strategy. Extensive simulation results have shown that the proposed scheme enlarges total throughput in comparison with STDMA inside each network, as well as non-STDMA scheme. Meanwhile, it achieves the lowest packet loss rate under heavy traffic load.

1 Introduction

With up to 7 GHz unlicensed bandwidth in most countries, 60-GHz millimetre-wave (mm-wave) communication shows great potential in wireless personal area networks (WPANs) and wireless local area networks (WLANs) [1]. The huge bandwidth provides tremendous capacity and flexibility, which enables multi-gigabit wireless transmissions. The applications of 60-GHz WPANs/WLANs are typically taking advantages of its instantaneous transfer and low latency characteristics, including wireless docking and uncompressed high-definition video streaming [2, 3]. Although mm-wave communication has been used in military and radar systems for decades, the progress of CMOS technology has made it commercially attractive for civil use recently [4]. Chipsets manufacturers such as Qualcomm have launched mm-wave products in volume production, some of which are already adopted in Dell laptops. Besides profit-making corporations, research institutes and standardisation bodies also pay high attention to 60-GHz band. Published standards include ECMA 387, IEEE 802.15.3c and IEEE 802.11ad [5]. Led by Intel and Qualcomm, an IEEE study group has been proposed for the next generation mm-wave communication system, and its goal is to achieve 30 Gb/s transmission rate or more. Meanwhile, mm-wave communication is also proposed as a promising technology for the 5th Generation mobile networking system [6, 7].

Since the path loss scales as λ^2, where λ refers to the carrier wavelength, mm-wave communication suffers much severer loss than existing low frequency wireless systems due to tiny wavelength [8, 9]. Therefore, directional beams formed by antenna arrays (beamforming) are utilised to compensate for such loss. The directivity may cause deafness problem [10], resulting in low possibility of conducting carrier sensing as in traditional WiFi networks. However, the interference between links in mm-wave system is much lower than that of low-frequency counterparts, where isotropic antennas are commonly used at the receiver. These factors pave way for spatial reuse to enhance overall network capacity [11]. The literature has been investigated the Media Access Control (MAC) protocols of spatial sharing without consideration of interference [12]. Nevertheless, the assumption of pseudo-wired link is not always the case. The existence of interference should not be ignored, as proved in [13].

Currently, IEEE 802.11ad standard has been widely acknowledged by manufacturers. Therefore, we focus on IEEE 802.11ad mm-wave system in this paper. Typically, in this standard, the system contains several networks, namely Personal Basic Service Sets (PBSSs), each of which comprises a central coordinator and multiple users, and transmits data in a sequence of non-overlapping time segments called Beacon Intervals (BIs). The standard supports spatial sharing with interference mitigation inside a PBSS [14]. However, normally the interference level among multiple networks is much less severer than that inside a network, which provides greater opportunity to schedule concurrent transmissions of links in different co-channel networks to achieve higher throughput gain. Therefore, it motivates the study of space-time division multiple access (STDMA) among multiple co-channel PBSSs in IEEE 802.11ad system. The contributions of our work are summarised as follows:

- We formulate the problem of STDMA scheduling among PBSSs as a mixed-integer non-linear programming (MINLP) problem, which takes the interference and characteristics of timing structure of multiple PBSSs in IEEE 802.11ad into consideration.
- We propose a heuristic STDMA scheme among multiple co-channel PBSSs. The main goal is to make full utilisation of spatial reuse between networks with reduced interference collision, and greedy principle is adopted to cut down spare time in each PBSS.
- We conduct simulations in the aspects of the network throughput and the packet loss rate under multiple traffic patterns, which demonstrates an obvious improvement in throughput and reliability performance by the proposed scheme, compared with using STDMA inside a PBSS or not adopting spatial reuse at all. In

addition, we further reveal the influence of interference level and threshold on the proposed scheme.

The rest of the paper is organised as follows. After presenting several related works in Section 2, we present the conventional WLAN network in IEEE 802.11ad standard, and provide a system model of spatial reuse among co-channel PBSSs in Section 3. In Section 4, the problem is mathematically stated and formulated. The following section proposes a scheduling scheme among multiple networks to achieve STDMA gain and mitigate interference. After that, simulation results are analysed in Section 6. Finally, we conclude the paper in Section 7.

2 Related works

Considerable works investigate the management of spatial reuse with interference mitigation in conventional cellular networks, e.g. soft frequency reuse [15, 16]. The goal is to enhance overall throughput and mitigate inter-cell interference. However, it is hard to employ those schemes directly in mm-wave WPANs/WLANs. With limited number of channel bands (four bands) and small coverage, co-channel interference is almost inevitable in 60-GHz communication. Meanwhile, the schemes of low frequency band are mostly based on omnidirectional antennas, which is not suitable in directional communication.

As for 60-GHz mm-wave communication, time division multiple access (TDMA) is typically used in IEEE 802.11ad standard. Some studies exploit spatial reuse in such system. In [12], a frame-based scheduling has been proposed, but the interference is ignored. Lan *et al.* [17] proposed a scheduling scheme sharing time slots for relay with direct transmission, which, however, requires extra control overhead and adds complexity to beamforming steering.

There are some works focusing on STDMA within a single mm-wave network, taking consideration of interference [18–22]. Such study includes centralised and distributed MAC protocols. Sum *et al.* [21] proposed a virtual time-slot allocation (VTSA) scheme based on centralised scheduling. The algorithm offers two optional methods, one of which selects the link with minimum channel interference with existing concurrent links, while the other one selects the link randomly. If the interference brought by the incoming link exceeds the threshold, the link would be allocated to the next frame. On the other hand, Singh *et al.* [22] presented a distributed MAC protocol to achieve implicit coordination by using history information. Each node employs learning rules to decide time-slot allocation based on its own memory. There is no doubt that spatial reuse scheduling inside a single PBSS could improve system throughput, but the interference still confines the number of concurrent transmissions.

If we extend the STDMA study with a group of co-channel networks, the interference level between them is usually much lower than that inside a network due to relatively far apart links, which provides greater potential for STDMA conduction. To the best of our knowledge, there are few works analysing interference between the two cases mentioned above or employing STDMA for the scenario of multiple co-channel networks. In IEEE 802.11ad, the biggest difference between conducting STDMA with interference mitigation inside a PBSS and among PBSSs is the timing structure. In a group of co-channel PBSSs, each network starts BI transmission in a different time, which brings great challenges to address the problem of STDMA scheduling.

3 System overview

3.1 Network architecture and timing

With reference in IEEE 802.11ad standard, PBSS acts as the fundamental network in 60-GHz system (similar to cellular network in conventional low frequency communication). One PBSS includes a PBSS control point (PCP) and multiple stations (STAs). The PCP allocates service period (SP), a contiguous time for data service transmission of a link, in each PBSS [23].

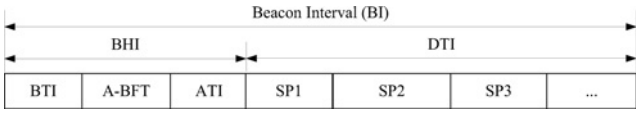

Fig. 1 *Timing structure of a BI in IEEE 802.11ad*

In IEEE 802.11ad, data are transmitted in units of BIs. A BI consists of Beacon Header Interval (BHI) and Data Transmission Interval (DTI). BHI is further divided into three parts: Beacon Transmission Interval (BTI), Association Beamforming Training (A-BFT) and Announcement Transmission Interval (ATI) [23], which is shown in Fig. 1. One or more Beacon frames are transmitted in BTI. Beamforming training is processed in A-BFT, and a request-response based management occurs in ATI, both of which are optional in Beacon frames. There is a single DTI in each BI, and it comprises multiple SPs, which are scheduled by the PCP for data transmission.

3.2 Interference and clustering mechanism

Although directional links are established in 60-GHz mm-wave system, interference cannot be ignored, due to limitations in antenna technology and the trend of network densification and so on [24]. In addition, interference level between PBSSs is much lower than that within a single PBSS. We assume a system containing three co-channel networks, each of which includes six devices. Antenna arrays with four elements are adopted by all devices. Constrained in a 10 m × 8 m cubicle room, the devices in each PBSS are uniformly distributed in a circular area with a radius of 3 m and overlapping between different PBSSs occasionally occurs. We establish a directional link between every two devices in the same PBSS, and the transmitter and the receiver of the link are randomly designated. When activating two independent links simultaneously, the SINR value for each link could be obtained. By recording all SINR values, the percentages of these values in multiple numerical intervals are shown in Table 1. The terms 'intra' and 'inter' show where the interference comes from, i.e. activating every two links in the same PBSS and in different PBSSs, respectively. Table 1 lists results in eight independent experiments, in each of which the position of all devices are updated according to the previous principal. Typically we regard a severe interference occurs when SINR value is less than 6 dB. It can be observed that the percentage of severe intra-PBSS interference is much larger than that of inter-PBSS interference, which is mainly due to the larger distance between links in different PBSSs than that in the same PBSS. When extending the number of experiments to 100, the average possibility that two links do not interfere with each other, i.e. are able to coexist for spatial reuse, becomes $77.96\%^2 \simeq 61\%$ for intra

Table 1 Interference level comparison between links within one PBSS and among multiple PBSSs

Experiment no.	SINR < 3 dB		3 dB ≤ SINR ≤ 6 dB		SINR > 6 dB	
	Intra, %	Inter, %	Intra, %	Inter, %	Intra, %	Inter, %
1	12.96	2.89	4.81	3.19	82.22	93.92
2	21.11	5.55	8.15	4.67	70.74	89.78
3	17.04	4.96	4.44	3.78	78.52	91.26
4	16.30	4.37	3.70	3.33	80.00	92.30
5	12.96	0.44	6.30	0.74	80.74	98.82
6	17.04	5.93	6.66	3.26	76.30	90.81
7	15.92	6.74	10.01	5.93	74.07	87.33
8	17.78	2.00	8.89	2.96	73.33	95.04
average result for 100 cases	15.03	4.47	7.00	3.53	77.96	92.01

IET Commun., 2016, Vol. 10, Iss. 4, pp. 425–434

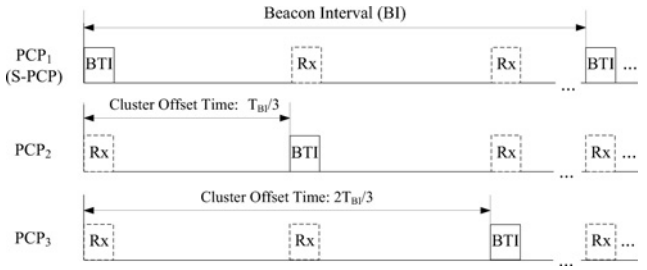

Fig. 2 *Example of cluster mechanism (three PCPs in a cluster)*

scenario, while $92.01\%^2 \simeq 85\%$ for inter scenario. Both of the coexisting possibilities decrease exponentially as the number of concurrent links grows. The results validate that conducting STDMA between PBSS is more promising to achieve throughput enhancement and interference mitigation than inside a PBSS.

In IEEE 802.11ad standard, clustering mechanism is adopted to improve interference mitigation among PBSSs. Typically a cluster includes a synchronisation PCP (S-PCP) and several member PCPs. Fig. 2 shows an example of clustering of three PBSSs. Two member PCPs (PCP_2 and PCP_3) shall select the same BI length as that of S-PCP (PCP_1). Each PCP gets a Beacon SP (BTI) to transmit frames that contain SP allocation information of current BI to other cluster PCPs, which should listen and not schedule or transmit any data during that period. Typically the BTI intervals between every two sequent PBSSs are equal. If severe interference results in low system throughput, the clustering mechanism suggests its PCPs to schedule transmissions in non-overlapping time periods to avoid interference.

3.3 STDMA among PBSSs

Spatial reuse within one PBSS is considered in current IEEE 802.11ad standard. Two SPs are allowed to use overlapped time period if there is little interference between corresponding links. In our system model, we extend this STDMA scheme to be conducted among multiple co-channel PBSSs, an example of which is shown in Fig. 3. In this scenario, any two devices in the same PBSS are able to establish a link. We assume that there are five links that have traffic demands in each PBSS, and each link requires a SP to transmit data. Links in the same coloured pattern means the interference level in this pair exceeds the threshold. For example, the communication of link between STA_{B2} and STA_{B1} in $PBSS_B$ is affected by that of link between PCP_A and STA_{A1} in $PBSS_A$. Therefore, the two links are painted with the same coloured pattern and cannot be allocated simultaneously. The scheduling result in Fig. 3 contains several consecutive time periods for spatial reuse, termed phases. The time lengths of SPs in the same phase are not necessarily the same. For example, there is a little spare time in phase 1 for B-SP2. The reason why we do not allocate B-SP4 right after B-SP2 is that it would cause more SPs overlapped (both interferences between A-SP4 and B-SP2, as well as between A-SP4 and B-SP4 have to be considered), and result in larger possibility of severe inter-PBSS interference. By adopting proper scheduling scheme, required SPs could be allocated in appropriate phases to achieve higher throughput gain.

4 Problem formulation

In this section, we assume that there are N co-channel PBSSs in the system, and the ith PBSS ($i = 1, 2, \ldots, N$) contains L_i directional links. The smaller the PBSS index, the earlier it starts transmission in the system. Since data transmissions are based on BI, the transmission demands matrix for each BI can be given as

$$\boldsymbol{D}(i,j) = \begin{cases} d_{ij} & j \le L_i, \quad i = 1, 2, \ldots, N, \\ 0 & \text{otherwise.} \end{cases} \tag{1}$$

The size of matrix $\boldsymbol{D}$ is $N \times L_{\max}$, where $L_{\max} = \max_i(L_i)$, and d_{ij} is the number of time slots needed to the required data transmission. We define the SP allocation for N PBSS, each contains a BI, as a schedule. The N BIs start sequently and the sequence is the same as that of the starting time of corresponding PBSSs. Each schedule

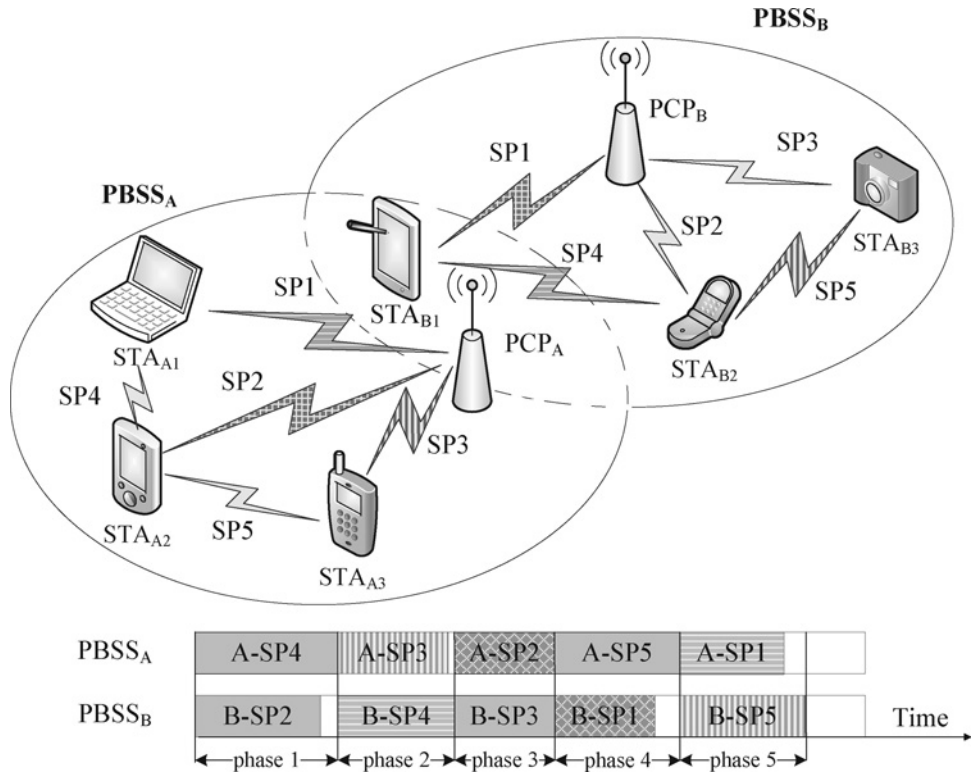

Fig. 3 *System model: spatial reuse and interference mitigation among co-channel PBSSs*

comprises S phases. Binary variable a_{ij}^s denotes whether the jth ($j = 1, 2, \ldots, L_i$) link in the ith PBSS are activated during the sth ($s = 1, 2, \ldots, S$) phase in the schedule. Define transmission matrix at the sth phase as $\boldsymbol{A}_s$, which has the same size as $\boldsymbol{D}$, and it is consisted of binary element a_{ij}^s. The allocated time for data transmission should be no smaller than traffic demands. Thus, we have the following constraint between $\boldsymbol{D}$ and $\boldsymbol{A}_s$ as

$$d_{ij} \le \sum_{s=1}^{S} \delta^s a_{ij}^s, \quad a_{ij}^s \in \boldsymbol{A}_s, d_{ij} \in \boldsymbol{D}, \tag{2}$$

where δ^s is the phase time, i.e. the maximum time duration of SPs among all PBSSs in the sth phase. We assume that each link gets at most one SP in every schedule to reduce overhead such as beamforming and tracking.

According to the timing structure of a cluster in IEEE 802.11ad, the relation between the phase time and starting time of each PBSS can be presented as follows

$$a_{ij}^s \cdot \sum_{t=1}^{s-1} \delta^t \ge \Omega_i \cdot a_{ij}^s, \quad \forall i, j, s. \tag{3}$$

Ω_i refers to the time duration in the schedule before the ith PBSS starts, i.e. the Cluster Offset Time in Fig. 2, where typically $\Omega_i = (i-1)T_{\mathrm{BI}}/N$ ($i = 1, 2, \ldots, N$) and T_{BI} is the duration of a BI [23]. Each PBSS should allocate its SP after Ω_i. Thus, the total time of all previous phases in the schedule is longer than Ω_i if a_{ij}^s is assigned as 1 in the current phase.

The signal-to-interference-plus-noise ratio (SINR) value is based on Friis propagation law [25]. For example, the received SINR value of link j in PBSS$_i$ when it is transmitted simultaneously with link y in PBSS$_x$ is defined as

$$\begin{aligned} \mathrm{SINR}_{x_y 2 i_j} &= \frac{P_{\mathrm{t}} G_{\mathrm{t}}(\theta_{\mathrm{t},ij}) g_{ij} G_{\mathrm{r}}(\theta_{\mathrm{r},ij})}{P_{\mathrm{t}} G_{\mathrm{t}}(\theta_{\mathrm{t},(ij,xy)}) g_{(ij,xy)} G_{\mathrm{r}}(\theta_{\mathrm{r},(ij,xy)}) + N_0 B}, \\ g_{ij} &= \frac{(4\pi\lambda)^2}{d_{ij}^2}, \quad g_{(ij,xy)} = \frac{(4\pi\lambda)^2}{d_{(ij,xy)}^2}, \\ & x \ne i, y = 1, 2, \ldots, L_x. \end{aligned} \tag{4}$$

P_{t} refers to the transmitted power, while $G_{\mathrm{t}}(\cdot)$ and $G_{\mathrm{r}}(\cdot)$ stand for the transmitted and received antenna gains, respectively; $\theta_{\mathrm{t},ij}$ and $\theta_{\mathrm{r},ij}$ are transmitted and received angles of link j in PBSS$_i$, respectively; $\theta_{\mathrm{t},(ij,xy)}$ and $\theta_{\mathrm{r},(ij,xy)}$ refer to the transmitted and received angles between the transmitter of link y in PBSS$_x$ and the receiver of link j in PBSS$_i$, respectively; g_{ij} and $g_{(ij,xy)}$ are attenuation factors of link j in PBSS$_i$, and the link between the transmitter of link y in PBSS$_x$ and the receiver of link j in PBSS$_i$, respectively, and d_{ij} and $d_{(ij,xy)}$ stand for distances between the transmitter and the receiver of the above two links independently. N_0 and B are power spectral density of white Gaussian noise and system bandwidth, respectively. If the SINR value exceeds the threshold, the corresponding links (link i and link j) in different PBSSs cannot coexist.

Combine the above discussion and analysis, the optimal scheduling problem can be formulated as follows. The goal of the optimal problem is to minimise the total scheduling time of all required data packets, and therefore to achieve the highest throughput

$$\min \sum_{s=1}^{S} \delta^s, \tag{5}$$

$$\text{s.t.} \quad \sum_{s=1}^{S} a_{ij}^s \in \{0, 1\} \quad \forall i, j, s; \tag{5a}$$

$$\sum_{s=1}^{S} a_{ij}^s = \begin{cases} 1 & d_{ij} > 0 \\ 0 & \text{otherwise} \end{cases} \quad \text{for all } i, j; \tag{5b}$$

$$\sum_{s=1}^{S} \delta^s \cdot a_{ij}^s \begin{cases} \ge d_{ij} & d_{ij} > 0 \\ = 0 & \text{otherwise} \end{cases} \quad \forall i, j; \tag{5c}$$

$$\sum_{j=1}^{L_i} a_{ij}^s \le 1 \quad \forall i, s; \tag{5d}$$

$$a_{ij}^s \cdot \sum_{t=1}^{s-1} \delta^t \ge \Omega_i \cdot a_{ij}^s \quad \forall i, j, s; \tag{5e}$$

$$a_{ij}^s \cdot \sum_{t=1}^{s} \delta^t \le (T_{\mathrm{DTI}} + \Omega_i) \cdot a_{ij}^s \quad \forall i, j, s; \tag{5f}$$

$$\begin{aligned} & a_{ij}^s + a_{xy}^s \le 1, \quad \text{if } \mathrm{SINR}_{x_y 2 i_j} \text{ or } \mathrm{SINR}_{i_j 2 x_y} \Gamma, \\ & \forall i, j, x, y, s \ (x \ne i); \end{aligned} \tag{5g}$$

$$a_{ij}^s + \hat{a}_{zw}^{\hat{s}} \le 1, \quad \text{if} \begin{cases} \mathrm{SINR}_{z_w 2 i_j} \text{ or } \mathrm{SINR}_{i_j 2 z_w} < \Gamma \\ T_{\mathrm{BI}} + \sum_{t=1}^{s-1} \delta^t - \sum_{\hat{t}=1}^{\hat{s}} \hat{\delta}^{\hat{t}} < 0 \\ T_{\mathrm{BI}} + \sum_{t=1}^{s} \delta^t - \sum_{\hat{t}=1}^{\hat{s}-1} \hat{\delta}^{\hat{t}} > 0 \end{cases} \tag{5h}$$

$$z = 1, 2, \ldots, N, \quad \text{and} \quad z \ne i, \quad \forall i, j, w, s, \hat{s}.$$

Equation (5) shows the binary constraint of a_{ij}^s. Equation (5b) restricts that 1 can be assigned to a_{ij}^s at most once at all phases. Constraint (5c) means the duration of the allocated SP should be no smaller than the demanded transmission time. Equation (5d) confines that no more than one link is activated in a particular network at phase s. Constraint (5e) illustrates unique timing structure of cluster in IEEE 802.11ad, as already shown in (3). Constraint (5f) shows that scheduling time in each PBSS should be no larger than the time length of a DTI, denoted as T_{DTI}, and DTI is the period for data transmission in BI. Constraint (5g) shows two links cannot be activated simultaneously if any of their SINR is smaller than threshold Γ, i.e. two concurrent transmissions should not severely interference with each other. In (5h), $\hat{a}_{zw}^{\hat{s}}$ refers to the binary variable in the phase $\hat{s}$ of the previous schedule, which can be regarded as constant in the problem. Two inequations in (5h) containing T_{BI} mean that phase $\hat{s}$ in the previous schedule and phase s in the current schedule has overlapping time period, thus links of different PBSSs within this overlapping area cannot interfere with each other, either. It can be further written as

$$\begin{aligned} & a_{ij}^s (T_{\mathrm{BI}} + \sum_{t=1}^{s-1} \delta^t - \sum_{\hat{t}=1}^{\hat{s}} \hat{\delta}^{\hat{t}})(T_{\mathrm{BI}} + \sum_{t=1}^{s} \delta^t - \sum_{\hat{t}=1}^{\hat{s}-1} \hat{\delta}^{\hat{t}}) \ge 0, \\ & \text{if } (\mathrm{SINR}_{z_w 2 i_j} \text{ or } \mathrm{SINR}_{i_j 2 z_w} > \Gamma) \text{ and } \hat{a}_{zw}^{\hat{s}} = 1. \end{aligned} \tag{6}$$

The optimisation problem (5) is a MINLP problem. Nevertheless, using linear relaxation, i.e. substituting $a_{ij}^s \cdot \delta^s$ with ξ_{ij}^s, $\sum_{t=1}^{s-1} \delta^t$ with γ^s, $a_{ij}^s \cdot \sum_{t=1}^{s-1} \delta^t$ with ζ_{ij}^s, and $a_{ij}^s \sum_{t=1}^{s} \delta^t \sum_{t=1}^{s-1} \delta^t$ with χ_{ij}^s, the problem is transformed into a mixed-integer linear programming (MILP) problem. Optimisation tools such as *lp_solver* and YALMIP are feasible to solve such problem [12].

We take the following example to interpret the problem. Consider a system of three co-channel PBSSs, each comprising of five links. A time slot lasts for 1 ms and each BI contains 100 time slots, thus we get $\Omega_1 = 0$, $\Omega_2 = 33$ and $\Omega_3 = 66$. We allocate 2 ms for BHI and 98 ms for DTI. For the first schedule, the demand matrix is

$$\boldsymbol{D} = \begin{bmatrix} 0 & 32 & 13 & 0 & 38 \\ 0 & 22 & 29 & 9 & 0 \\ 19 & 8 & 20 & 0 & 0 \end{bmatrix}. \tag{7}$$

Assuming that three pairs of links cannot coexist, and interference

constraint is as follows

$$\begin{cases} a_{15} + a_{32} \le 1, \\ a_{14} + a_{25} \le 1, \\ a_{22} + a_{33} \le 1. \end{cases} \tag{8}$$

We solve the optimal problem using YALMIP toolbox. The schedule $\boldsymbol{S}_{ch}$ is shown in the following equation (see (9))

It can be observed that STDMA is conducted in most phases. It takes 5 phases and 117 time slots altogether to finish all required transmissions, which otherwise costs 187 time slots if no STDMA is adopted.

In the formulated MILP optimisation problem, the number of decision variables is $\mathcal{O}(SNL_{\max})$ and the number of constraints is $\mathcal{O}(S(NL_{\max})^2)$. However, it is time-consuming to solve optimisation problem, which is unacceptable for practical mm-wave WLAN system. Therefore, it is necessary to propose a STDMA scheduling scheme with low complexity.

5 STDMA scheduling with interference mitigation among PBSSs

5.1 Training and interference report

Before scheduling, training is conducted by PCPs in a cluster, which takes time of one or several consecutive BIs. During the process, only one link conducts packet transmission at one SP in DTI, in the meanwhile all other links within the same PBSS and in other PBSSs record received SINR values without changing their original beam direction. After a certain period of training, a database of inter-PBSS co-channel interference (ICI) for each PBSS is established, namely ICI matrix

$$\begin{aligned} \mathrm{ICI}_{A2B}(\mu, \nu) &= \begin{cases} 0 & \mathrm{SINR}_{A_\mu 2B_\nu} > \Gamma, \\ 1 & \mathrm{SINR}_{A_\mu 2B_\nu} \le \Gamma; \end{cases} \\ & \mu = 1, 2, \ldots, L_A, \nu = 1, 2, \ldots, L_B, \\ \mathrm{ICI}_{A2B}(\mu, \nu) &= 0; \quad \mu = 0 \text{ or } \nu = 0. \end{aligned} \tag{10}$$

Element 1 in the matrix shows that the SINR value is small, i.e. interference generated by the μth link in PBSS_A to the νth link in PBSS_B exceeds the threshold, which needs to be mitigated. Since PCPs are able to exchange information in a cluster, the ICI matrix between every two PBSSs can be established and then known by each PCP. The S-PCP could start training process again according to the network performance, e.g. the throughput falls sharply. Since the mechanism of spatial reuse within each PBSS requires similar training process in IEEE 802.11ad standard, there is little extra overload of inter-PBSS spatial reuse compared with intra-PBSS scenario.

5.2 STDMA scheduling algorithm among multiple PBSSs

Without loss of generality, we consider a cluster comprising of N co-channel PBSSs, which are denoted as $P_1, P_2, \ldots, P_N$ according to the sequence of transmission. Each PBSS is composed of a PCP and several STAs. There are $L_1, L_2, \ldots, L_N$ links that have traffic demands in $P_1, P_2, \ldots, P_N$, respectively. The SP allocation of P_i ($i = 1, 2, \ldots, N$) is based on the previously finished SP scheduling in other $(N-1)$ PBSSs, and the algorithm is performed in units of BI.

The STDMA scheduling in the proposed algorithm is based on the following rules: (i) the concurrent links of different PBSSs do not interfere with each other; and (ii) in the same phase, the length of the newly allocated SP should not exceed the maximum length of previous scheduled SPs of other PBSSs. Since the scheduling in each network is based on the same rule, Algorithm 1 (see Fig. 4) shows the scheduling procedure in P_N as an example. The input and output sets are depicted as follows:

- *Input:* Denote the SP set in P_N as $T_N = \{t_{N1}, t_{N2}, \ldots, t_{NL_N}\}$, the element of which is the transmission time of required links in P_N in non-increasing order. Denote the link set of P_N as $V_N = \{v_{N1}, v_{N2}, \ldots, v_{NL_N}\}$, where v_{Nk} ($k = 1, 2, \ldots, L_N$) refers to the index of link with transmission time of t_{Nk}. Similarly, we define the SP set and link set of P_n ($n = 1, 2, \ldots, N-1$) as $T_n = \{T_{n1}, T_{n2}, \ldots, T_{nM_n}\}$ and $V_n = \{v_{n1}, v_{n2}, \ldots, v_{nM_n}\}$, respectively. It is important to note that T_n denotes the part of finished scheduling time set in P_n that is partitioned from the beginning time of DTI of the current BI in P_N.
- *Output:* Denote the output link set of P_N as $W_N = \{\{w_{N1}, \tilde{w}_{N1}\}, \{w_{N2}, \tilde{w}_{N2}\}, \ldots\}$, where the elements refer to the indices of links. The set illustrates the transmission sequence of every link after STDMA scheduling in P_N, and w_{N1} and $\tilde{w}_{N1}$ are transmitted subsequently in the same phase. Corresponding SP sets include $TP_N = \{\{tp_{N1}, \widetilde{tp}_{N1}\}, \{tp_{N2}, \widetilde{tp}_{N2}\}, \ldots\}$ and $TS_N = \{ts_{N1}, ts_{N2}, \ldots\}$. Specifically, in the kth phase of P_N, the total time of the SP is ts_{Nk}, while the time to transmit data is tp_{Nk}. In the same phase, $\widetilde{tp}_{Nk}$ refers to the transmission time for an additional short inserted SP after tp_{Nk}, and it can be set as 0 if there is no qualified short SP. If there is no qualified link during the kth SP, w_{Nk}, $\tilde{w}_{Nk}$, tp_{Nk} and $\widetilde{tp}_{Nk}$ are both set as 0, indicating no data is transmitted in this SP.

In Algorithm 1 (Fig. 4), lines 1 and 2 deal with the situation where all transmissions in P_1 have been accomplished before the starting time of DTI of the current BI in P_N. Then we could redefine $P_2, P_3, \ldots, P_N$ as $P_1, P_2, \ldots, P_{N-1}$, and set N as $N-1$, where the algorithm for a system comprising of $(N-1)$ PBSSs is recursively invoked. Otherwise the algorithm is shown in lines 3–32, the corresponding flowchart of which is depicted in Fig. 5. Line 5 constrains the sequence of SP scheduling: We first deal with the phases that are overlapped by all N PBSS BIs. After the last overlapped phase from P_1 to P_N, overlapped phases in P_2 to P_N are considered and so forth. The judgement of a qualified candidate is given in line 10. Its time duration should not exceed the maximum time duration of concurrent SPs in other PBSSs, neither should the interference between concurrent links and the candidate link exceed the ICI threshold. Line 12 shows that we stop searching once a qualified SP is found. Owing to non-increasing order of elements in T_N, the first qualified SP we choose owns the maximum time duration among all candidates that satisfy the conditions in line 10, which helps save computational time. To further explore spatial reuse, we insert short required SPs into an existing scheduled phase period if there is enough spare place at the beginning T_{BI}/N time of the DTI, as shown in lines 20–29. After selecting and allocating required SPs to the overlapped phases between P_{N-1} and P_N, we put the

$$\begin{aligned} \boldsymbol{S}_{ch} = \sum_{s=1}^{S} \delta^s \boldsymbol{A}_s = 38 \begin{bmatrix} 0 & 0 & 0 & 0 & 1 \\ 0 & 0 & 0 & 0 & 0 \\ 0 & 0 & 0 & 0 & 0 \end{bmatrix} + 32 \begin{bmatrix} 0 & 1 & 0 & 0 & 0 \\ 0 & 0 & 1 & 0 & 0 \\ 0 & 0 & 0 & 0 & 0 \end{bmatrix} + 20 \begin{bmatrix} 0 & 0 & 1 & 0 & 0 \\ 0 & 0 & 0 & 1 & 0 \\ 0 & 0 & 1 & 0 & 0 \end{bmatrix} \\ + 22 \begin{bmatrix} 0 & 0 & 0 & 0 & 0 \\ 0 & 1 & 0 & 0 & 0 \\ 1 & 0 & 0 & 0 & 0 \end{bmatrix} + 8 \begin{bmatrix} 0 & 0 & 0 & 0 & 0 \\ 0 & 0 & 0 & 0 & 0 \\ 0 & 0 & 1 & 0 & 0 \end{bmatrix}. \end{aligned} \tag{9}$$

Algorithm

1: **if** ($T_1 = \emptyset$) **then**
2: Use Algorithm for system comprising $(N-1)$ PBSSs;
3: **else**
4: $m_{temp} \leftarrow 1$;
5: **for** $r = 1 : N-1$ **do**
6: **for** $m = m_{temp} : M_r$ in T_r **do**
7: Set $q = r, r+1, \cdots, N-1$;
8: $w_{Nm} \leftarrow 0, \tilde{w}_{Nm} \leftarrow 0, tp_{Nm} \leftarrow 0, \tilde{tp}_{Nm} \leftarrow 0$;
9: **for** each t_{nk} in T_N **do**
10: **if** $(v_{Nk} \in \mathbf{V}_N) \& (t_{Nk} \leq t_{rm}) \& (\mathbf{ICI}_{P_q 2 P_N}(v_{qm}, v_{Nk}) = 0) \& (\mathbf{ICI}_{P_N 2 P_q}(v_{Nk}, v_{qm}) = 0)$ **then**
11: $w_{Nm} \leftarrow v_{Nk}, \ tp_{Nm} \leftarrow t_{Nk}$;
12: $T_N \leftarrow T_N - \{t_{Nk}\}, V_N \leftarrow V_N - \{v_{Nk}\}$; **break** ;
13: **end if**
14: **end for**
15: $ts_{Nm} \leftarrow t_{rm}$;
16: $m_{temp} \leftarrow m_{temp} + 1$;
17: **end for**
18: **end for**
19: **end if**
20: Select ts_{N1} to ts_{NF} in the first T_{BI}/N time;
21: **for** $f = 1 : \ F$ **do**
22: **for** each t_{Nk} in T_N **do**
23: **if** $(t_{Nk} \leq ts_{Nf} - tp_{Nf})$ and link k in P_N satisfy the same
24: interference constraint (Line 10) as w_{Nf} **then**
25: $\tilde{w}_{Nf} \leftarrow v_{Nk}, \ \tilde{tp}_{Nf} \leftarrow t_{Nk}$;
26: $T_N \leftarrow T_N - \{t_{Nk}\}, V_N \leftarrow V_N - \{v_{Nk}\}$; **break**;
27: **end if**
28: **end for**
29: **end for**
30: $TP_N \leftarrow \{\{tp_{N1}, \tilde{tp}_{N1}\}, \cdots, \{tp_{NM_{N-1}}, \tilde{tp}_{NM_{N-1}}\}, T_N\}$;
31: $TS_N \leftarrow \{ts_{N1}, ts_{N2}, \cdots, ts_{NM_{N-1}}\}, T_N]$;
32: $W_N \leftarrow \{\{w_{N1}, \tilde{w}_{N1}\}, \cdots, \{w_{NM_{N-1}}, \tilde{w}_{NM_{N-1}}\}, V_N\}$.

Fig. 4 *STDMA scheduling algorithm for P_N*

remaining SPs of P_N (in their original descending sequence) after those scheduled ones, as shown in lines 30–32.

5.3 Example

We consider the same example as shown in Section 4, i.e. using the same demand matrix and interference constraints in (7) and (8). Fig. 6 shows the first transmission schedule by adopting the proposed algorithm. The black number in each phase represents the actual transmission time of each required SP, and the number in bracket stands for the idle time in this phase. After accomplishing the SP allocation of the first BI in P_1 and P_2, the scheduling procedure in P_3 (shown in the bottom of Fig. 6) is depicted as follows.

According to the third row of demand matrix in (7), we obtain the required transmission time for each SP of P_3 in non-increasing order: $T_3 = \{20, 19, 8\}$ ms, and corresponding link index: $V_3 = \{3, 1, 2\}$. Based on the overlapped phases between P_2 and P_3, we have $T_2 = \{4, 9, 22\}$ ms and $V_2 = \{3, 4, 2\}$. Similarly, $T_1 = \{4, 13\}$ ms and $V_1 = \{2, 3\}$. The time length of the first phase in P_3 is 4 ms. Since there is no non-zero element in T_3 that is less than or equal to 4, nothing is allocated in the first 4 ms of DTI in P_3, leaving it as an idle phase. The second phase in P_3 is overlapped by both P_1 and P_2. The time length of the allocated SP should not exceed the maximum duration of the phase, i.e. 13 ms. In the meanwhile, it should be able to coexist with links in the concurrent phase, i.e. link 3 in P_1 and link 4 in P_2. Therefore, link 2 becomes the only qualified link that satisfies the time duration and interference constraint in line 10 of Algorithm 1 (Fig. 4). Its corresponding SP is allocated to the second phase, with 8 ms transmitting data and 5 ms of spare time. In the third phase, there is no overlapped SPs between P_1 and P_3, and thus only the concurrent SP in P_2 needs to be considered. Although link 1 seems less appealing compared with link 3 in P_3 due to smaller SP time length, it becomes the best qualified candidate for the third phase because it could coexist with link 2 in P_2 while link 3 could not according to interference constraints in (8).

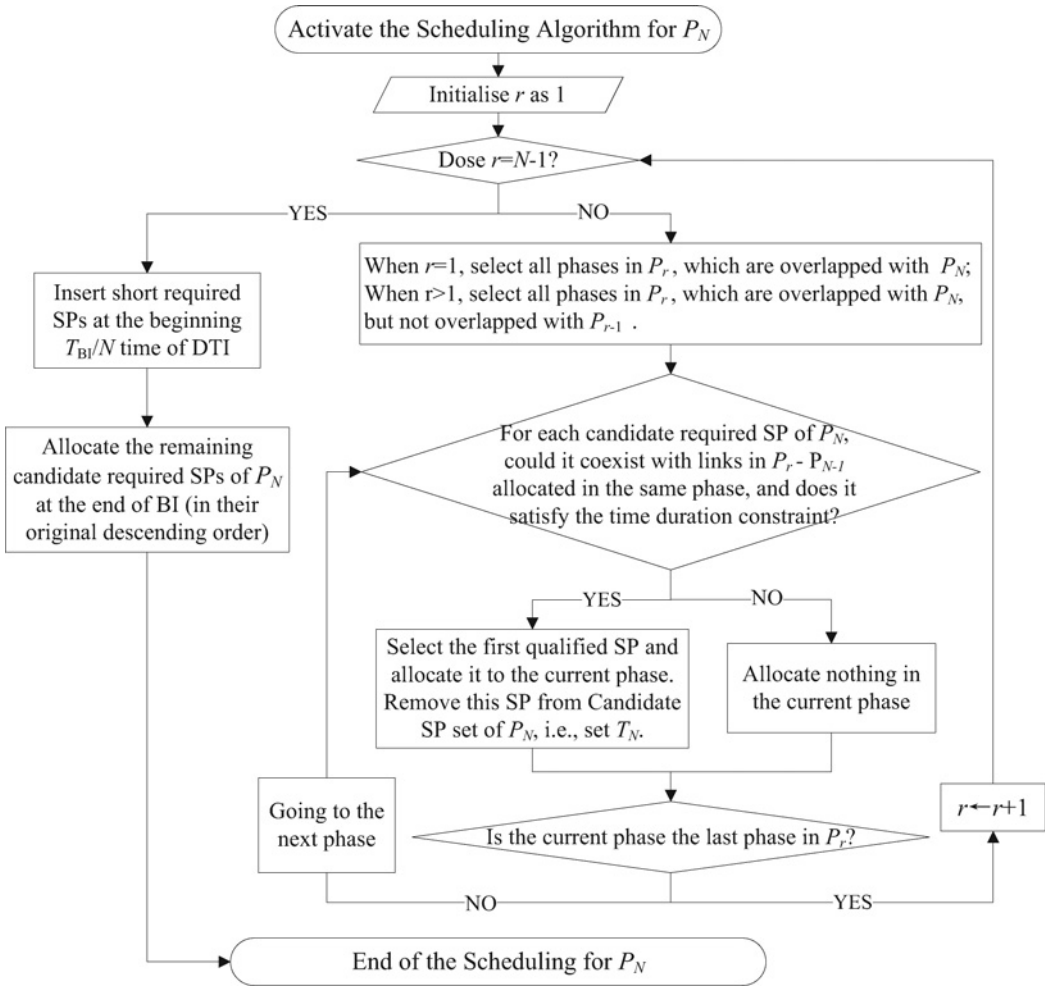

Fig. 5 *Flowchart of the proposed STDMA scheduling algorithm for P_N*

Finally, the SP for link 3 is allocated as the last SP in P_3 without any restriction since there is no overlapped part between three PBSSs in the current schedule. There is no available short SP inserted, and the output sets of P_3 could be written as: $W_3 = \{0, 2, 1, 3\}$, $TP_3 = \{0, 8, 19, 20\}$ ms and $TS_3 = \{4, 13, 22, 20\}$ ms, representing the transmission sequence in P_3 is {idle, link 2, link 1, link 3}, actual data transmission time is {0, 8, 19, 20} ms, and the time length of each phase is {4, 13, 22, 20} ms. If there is an extra traffic demand: $d_{35} = 4$, this short SP (link 5 in P_3) can then be allocated in the second phase right after link 2 in the schedule according to lines 20–29 in Algorithm 1 (Fig. 4), i.e. $\widetilde{tp}_{32} = 4$ ms and $\tilde{w}_{32} = 5$. After that, the scheduling for next BI (BI 2) of P_1 shall be based on SP allocation of previous BI (BI 1) of P_2 and P_3. By utilising the STDMA scheduling algorithm, 5 phases and 125 time slots are taken to finish all the traffic transmissions in the first schedule, which takes 5 extra time slots than using the MILP optimisation problem.

To investigate the gap between performance of MILP solution and our proposed algorithm, we adopt the same network structure as the above example, and conduct 100 independent experiments to obtain

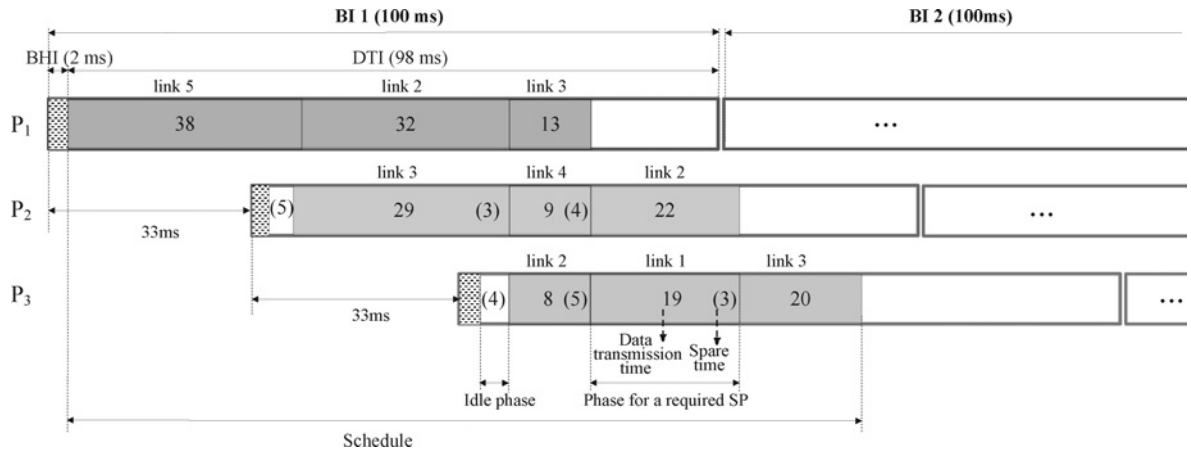

Fig. 6 *Example of the first schedule of three co-channel PBSSs adopting STDMA scheduling algorithm*

allocations for 100 schedules. Since the simulation time of MILP may become extraordinarily long with the increase of the number of phases, we randomly select three to four links in each PBSS to receive transmission requests in each experiment. Interference is randomly assumed based on the percentage results in Section 3. We simply assume the transmission rate for each link is the same, and data arrival rate is one-fifth of the link rate, i.e. the average time length of each request is around 20 ms. Since MILP could allocate data transmission in a shorter time, and thus transmit more data in a fixed-length schedule. The average throughput by using a heuristic algorithm is 5.8% less than that by using MILP. In around half (51%) of experiments, both methods accomplish all requests within the time length of one schedule, where on average it takes 135.8 ms to finish data transmission by adopting MILP and 146.0 ms by using the proposed algorithm.

Similar to MILP problem, the storage space for ICI matrix of the proposed algorithm is $\mathcal{O}(\sum_{i=1,h>i} 2L_iL_h)$, where $i = 1, 2, \ldots, N-1$ and $h = 2, 3, \ldots, N$. For each PBSS P_i, the computational times of the proposed scheme include the times for sorting T_i in descending order and for comparing and judging whether the current SP satisfies the time duration and interference constraint, which are $\mathcal{O}(L_i \log L_i)$ and $\mathcal{O}(L_i(L_i + 2L_i(N-1)))$, respectively. Since $L_i \leq L_{\max}$, the complexity for scheduling N PBSSs is $\mathcal{O}((NL_{\max})^2)$. The MATLAB running time for the above 100 experiments by using the heuristic algorithm is around $1/10^4$ of that by solving a MILP problem in a desktop computer with an Intel Core CPU with 3.4 GHz processor speed and 8 GB RAM, which makes it much more competitive in practical networks despite the minor performance loss.

6 Performance evaluation

6.1 Simulation setup

(i) *Network setting:* In the simulation, we assume a system comprising of three co-channel PBSSs, each of which contains six devices and link establishment is available between any two devices. Accordingly, a maximum of three concurrent transmissions is allowed inside a PBSS adopting STDMA inside each network, or among three PBSSs in our proposed scheme. The transmission takes place in a cubicle room of 10 m × 8 m. Each PBSS has a fixed central point as the location of its PCP. Other devices are uniformly distributed within a circular area around the PCP. When the coordinate lies outside of the room space, it is then constrained to the edge of the room. The simulated network is depicted in Fig. 7, which contains four randomly generated cases which contains three randomly generated cases. In each case, three central points are (3, 2), (5, 6) and (7, 3) denoted by stars, and the radius of the circular range is $R = 3$ m. It can be observed from the figure that devices in a PBSS are relatively close to each other, but overlapping of PBSSs occasionally occurs, which is likely to result in interference.

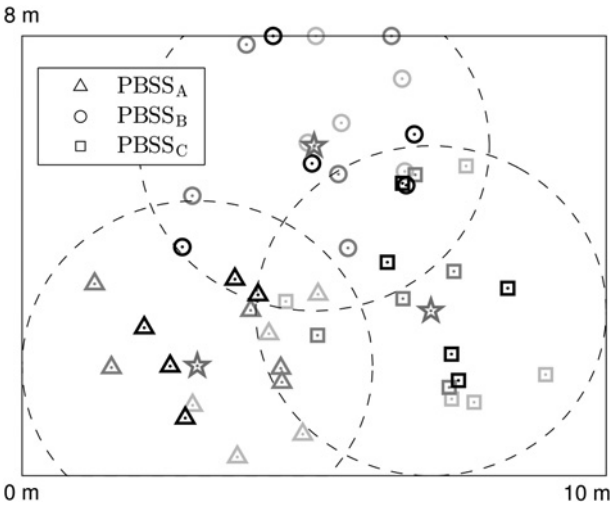

Fig. 7 *Simulated network in a cubicle room (three random cases: distribution of each case is depicted by markers with black, grey and light grey edge respectively, and stars stand for PCPs in each PBSS)*

(ii) *Channel and antenna model:* To simplify the simulation, only line of sight channel is considered in each link. The main parameter settings are listed in Table 2. Uniform linear phased antenna array is adopted at each device. We select a realistic antenna model to generate beams pointing to certain directions. The antenna weight vector is written as

$$\boldsymbol{w}(\tilde{n}) = \mathrm{e}^{-\mathrm{j}(2\pi/\lambda)d\cos\theta_0}, \quad \tilde{n} = 0, 1, 2, \ldots, \tilde{N}-1, \tag{11}$$

where d is the distance between antenna elements, $d = \lambda/2$; $\tilde{n}$ is the index of antenna element; $\tilde{N}$ is the number of elements in the antenna array; and θ_0 refers to the angle of the desired main beam direction [26]. According to the above settings, ICI matrix is generated. The threshold of SINR value is set as 6 dB. Under heavy traffic load, every PBSS discards extra required packets in each BI, to avoid system congestion.

6.2 Comparison with existing schemes

In this subsection, three scheduling schemes are considered. We compare our proposed scheme, termed inter-STDMA, with the following two benchmarks:

- *Intra-STDMA scheme:* STDMA scheme in [21] is used in each PBSS, but there is no spatial reuse among different networks. To simplify simulation, each PBSS uses its first (T_{BI}/N) time of DTI to conduct STDMA.
- *Non-STDMA scheme:* In this scenario, no STDMA scheduling is conducted in a PBSS or among PBSSs. At most one link is communicating in the whole system at one time and no interference needs to be considered.

The traffic model is set as Poisson model, in which the data demand for each link obeys Poisson distribution in each time slot [27]. Meanwhile, we adopt two traffic patterns: *uniform* and *non-uniform*. In the *uniform* pattern, each link in a PBSS has the same opportunity for transmission, while in the *non-uniform* pattern, a subset of links get higher chance to transmit, and leave others with lower packet arrival rate. The average arrival rate of both patterns is set to be the same.

In our MATLAB simulation, 100 random network distributions are generated, each of which contains 100 BI transmissions for every PBSS. Each BI lasts for 100 ms, containing 2 ms for BHI, and 98 ms for DTI. In *non-uniform* pattern, the arrival rate of 50% of the links is 1.5ρ while that for the other links is 0.5ρ, where ρ is the arrival rate of each link in *uniform* pattern. The corresponding throughput and packet loss rate of three cases under two traffic patterns are listed below. Although the performance of throughput and reliability in *uniform* pattern is slightly better than that of *non-uniform* pattern, the curve trend and relation between the three schemes to keep the same.

Table 2 Parameters of channel setting

Parameter	Value
Tx power	10 dBm
noise spectral density	−174 dBm/Hz
bandwidth	1.76 GHz
wavelength	5 mm
number of transmit antenna elements (N_t)	8
number of receive antenna elements (N_r)	8
noise figure	5 dB
other loss	5 dB

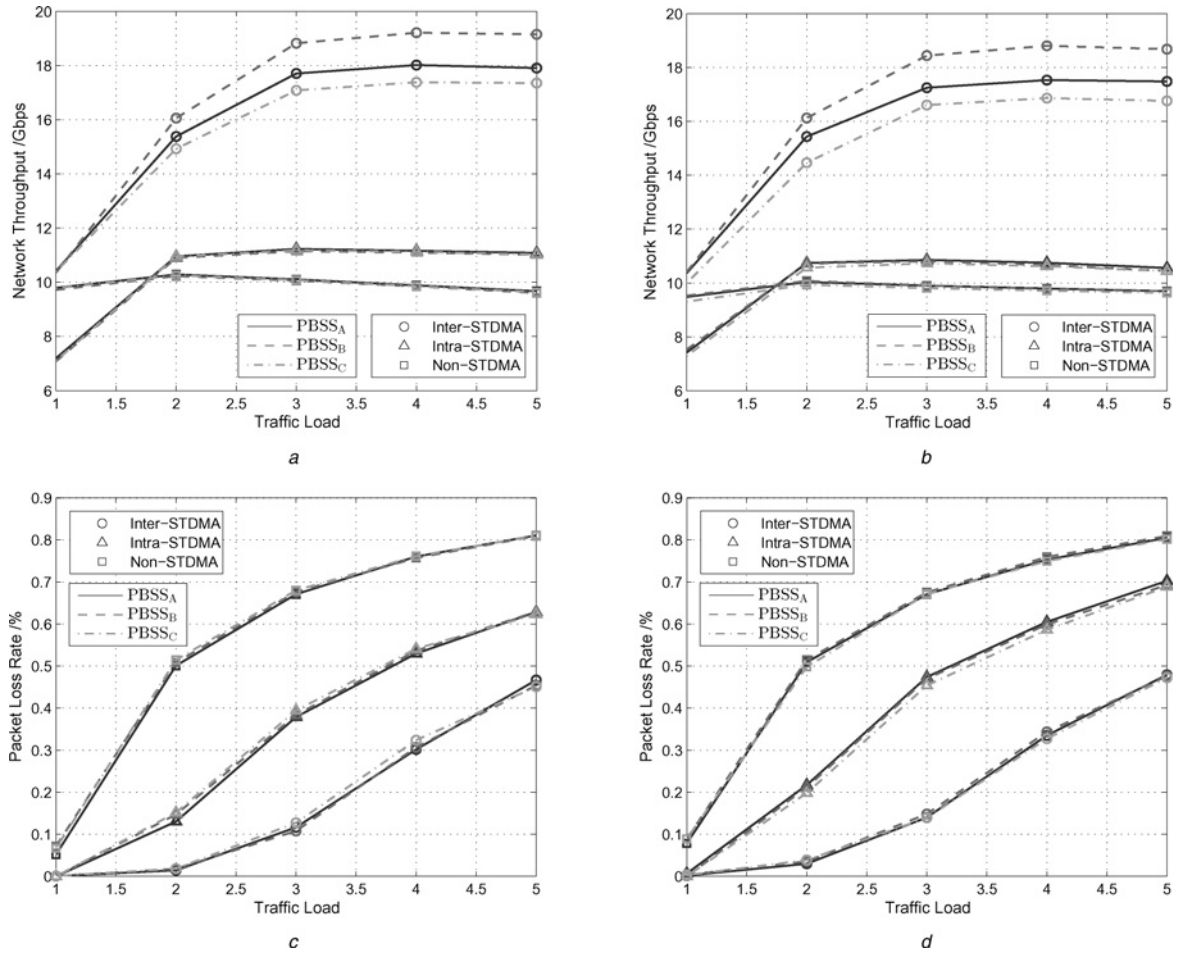

Fig. 8 *Network throughput and average packet loss rate of three scheduling schemes under uniform and non-uniform Poisson patterns*

a Network throughput (uniform Poisson)
b Network throughput (non-uniform Poisson)
c Packet loss rate (uniform Poisson)
d Packet loss rate (non-uniform Poisson)

6.2.1 Throughput: In this part, the system throughput is obtained according to the real SINR value according to distance and beam angle and so on. Figs. 8*a* and *b* manifest throughput of each PBSS under three schemes. The *x*-axis refers to the normalised traffic load. For example, a traffic load 3 means the traffic requirements is three times of the capacity of a single directional link. The traffic load is equal to ρL_{total}, where L_{total} is the total number of links in the system.

By using the proposed inter-STDMA scheme, the throughput goes up quickly and almost keeps steady after a traffic load 3, with around 18 Gb/s in *uniform* pattern and 17 Gb/s in *non-uniform* pattern. The throughput of each PBSS adopting intra-STDMA is shown by the line with triangles. Although it allows at most three links working at the same time inside a PBSS, it can be observed that the throughput almost peaked when the traffic load is 2 due to larger interference inside a PBSS than among different PBSSs. It is hard to find three links with little interference between each other inside a single PBSS. The throughput of intra-STDMA only achieves approximately 66% of that adopting inter-STDMA scheme. It is undoubted that non-STDMA achieves the least throughput except light traffic load 1, where it is higher than that of intra-STDMA. The reason is that all transmission demands can be accomplished in a short time. Therefore, data rate is higher in non-interference scenario.

6.2.2 Reliability: The packet loss rate performance under the three schemes is shown in Figs. 8*c* and *d*. In all cases, packet loss rate goes up with the increase of traffic load. There is no doubt that non-STDMA scheme achieves the largest packet loss rate, because it utilises the least time and space for data transmission. Over 80% of packets are lost during heavy traffic load in both patterns. The rates of intra-STDMA scheme are in the middle and those of inter-STDMA scheme are the least, which means the proposed scheme gets the highest reliability among the three cases. The proposed scheme can guarantee less than 5% packets loss when traffic loads are 1 and 2, and is still able to transfer more than half of demanded data under heavy traffic load 5.

6.3 Effects of ICI level and ICI threshold

The previous subsection shows the throughput enhancement by adopting inter-STDMA scheme between co-channel PBSSs. The effects of ICI level and ICI threshold for the proposed scheme under *uniform* Poisson pattern are analysed in this part.

High ICI level means the interference among PBSSs is severe, and vice versa. According to the network settings, the interference level between different links varies when changing radius R. Fig. 9*a* illustrates the average throughput of three PBSSs under different ICI levels. As R increases, the throughput drops due to severer overlapping between different PBSSs. It can be noticed that the effect of the ICI level to the throughput becomes smaller when R is relatively bigger, where devices in different PBSSs get closer and ICI level becomes sufficiently high. The dotted lines depict the throughput performance in the scenario of four antenna elements at both the transmitter and receiver sides. Since the beam is wider and less directed, interference becomes severer, which results in around 30% loss in throughput under the same network distribution.

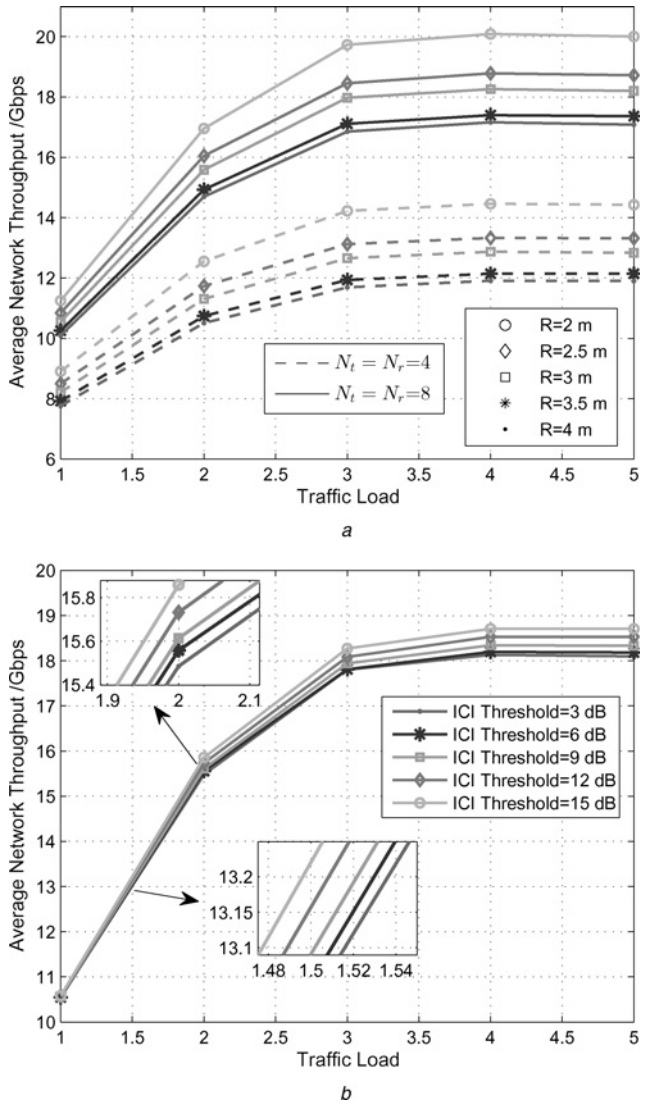

Fig. 9 *Effects of ICI level and ICI threshold to the Inter-STDMA scheme*
a Effects of ICI level
b Effects of ICI threshold

ICI threshold determines the number of elements 0 in ICI matrix, and affects the number of links that cannot be allocated to the overlapping time period. The average throughput performance of three PBSSs under different ICI thresholds is shown in Fig. 9*b*. Larger threshold guarantees less interference between allocated concurrent links, which achieves higher system throughput. However, the effect of ICI threshold is not as obvious as that of ICI levels.

7 Conclusion

Since phased antenna arrays are adopted in 60-GHz mm-wave communication system, directivity paves the way for spatial reuse. According to the statistical results, interference among co-channel PBSSs are much less severer than that inside a single PBSS, which is better for STDMA scheduling. An IEEE 802.11ad-based-STDMA scheduling scheme among PBSSs has been proposed in this paper. Through SINR measurement in the training process, PCPs in a cluster exchange information and then establish a database of interference, i.e. ICI matrix. By using previous knowledge, each PCP allocates SP based on greedy principle and mutual interference avoidance. When compared with STDMA scheme within PBSS and non-STDMA scheme, the extensive results have shown that our proposed algorithm achieves more throughput gain and less packet loss rate at different levels of traffic load.

8 Acknowledgments

This work was partially supported by the National Natural Science Foundation of China (NSFC) under grant nos. 61201189 and 61132002, National High Tech (863) Projects under grant no. 2011AA010202, Research Fund of Tsinghua University under grant nos. 2011Z05117 and 20121087985, and Shenzhen Strategic Emerging Industry Development Special Funds under no. CXZZ20120616141708264.

9 References

1 Huang, K., Wang, Z.: 'Millimeter wave communication systems' (Wiley, 2011)
2 Nechayev, Y.I., Wu, X., Constantinou, C.C., *et al.*: 'Millimetre-wave path-loss variability between two body-mounted monopole antennas', *IET Microw. Antennas Propag.*, 2013, **7**, (1), pp. 1–7
3 Yong, S.K., Xia, P., Valdes-Garcia, A.: '60 GHz Technology for Gbps WLAN and WPAN: from theory to practice' (Wiley, 2011)
4 Singh, S., Ziliotto, F., Madhow, U.: 'Blockage and directivity in 60 GHz wireless personal area networks: from cross-layer model to multihop MAC design', *IEEE J. Sel. Areas Commun.*, 2009, **27**, (8), pp. 1400–1413
5 Charfi, E., CHaari, L., Kamoun, L.: 'PHY/MAC enhancements and QoS mechanisms for very high throughput WLANs: a survey', *IEEE Commun. Sur. Tutor.*, 2013, **15**, (4), pp. 1714–1735
6 Roh, W., Seol, J.-Y., Park, J., *et al.*: 'Millimeter-wave beamforming as an enabling technology for 5G cellular communications: theoretical feasibility and prototype results', *IEEE Commun. Mag.*, 2014, **52**, (2), pp. 106–113
7 Dehos, C., Gonzalez, J.L., Domenico, A.D., *et al.*: 'Millimeter-wave access and backhauling: the solution to the exponential data traffic increase in 5G mobile communications systems', *IEEE Commun. Mag.*, 2014, **52**, (9), pp. 88–95
8 Yang, K., Huang, S.G., Zhu, J.H., *et al.*: 'Transmission of 60 GHz wired/wireless based on full-duplex radio-over-fibre using dual-sextupling frequency', *IET Commun.*, 2012, **6**, (17), pp. 2900–2906
9 Molisch, A.: 'Wireless communication' (Wiley, 2011)
10 Gong, M.X., Akhmetov, D., Want, R., *et al.*: 'Directional CSMA/CA protocol with spatial reuse for mmWave wireless networks'. Proc. GLOBECOM, Miami, FL, USA, December 2010, pp. 1–5
11 Serbetli, S., Yener, A.: 'Beamforming and scheduling strategies for time slotted multiuser MIMO systems'. Proc. Thirty-Eighth Asilomar Conf. on Signals, Systems and Computers, Pacific Grove, CA, USA, November 2004, pp. 1227–1231
12 Son, I.K., Mao, S., Gong, M.X., *et al.*: 'On frame-based scheduling for directional mmwave WPANs'. Proc. INFOCOM, Orlando, FL, USA, March 2012, pp. 2149–2157
13 Maltsev, A., Maslennikov, R., Maltsev, A., *et al.*: 'Performance analysis of spatial reuse mode in millimeter-wave WPAN systems with multiple links'. Proc. PIMRC, Cannes, France, September 2008, pp. 1–4
14 Chen, Q., Peng, X., Yang, J., *et al.*: 'Spatial reuse strategy in mmwave WPANs with directional antennas'. Proc. GLOBECOM, Anaheim, CA, USA, December 2012, pp. 5362–5367
15 Qian, M., Hardjawana, W., Li, Y., *et al.*: 'Inter-cell interference coordination through adaptive soft frequency reuse in LTE networks'. Proc. WCNC, Paris, France, April 2012, pp. 1618–1623
16 Daeinabi, A., Sandrasegaran, K., Zhu, X.: 'Survey of intercell interference mitigation techniques in LTE downlink networks'. Proc. ATNAC, Queensland, Australia, November 2012, pp. 1–6
17 Lan, Z., Wang, J., Gao, J., *et al.*: 'Directional relay with spatial time slot scheduling for mmwave WPAN systems'. Proc. VTC-Spring, Taipei, Taiwan, May 2010, pp. 1–5
18 Sum, C.-S., Lan, Z., Rahman, M.A., *et al.*: 'A multi-Gbps millimeter-wave WPAN system based on STDMA with heuristic scheduling'. Proc. GLOBECOM, Honolulu, Hawaii, December 2009, pp. 1–6
19 Yan, G., Liu, D.: 'A simple adaptive STDMA scheduling scheme in mmwave wireless networks'. Proc. ICCCAS, Chengdu, China, November 2013, pp. 159–163
20 Sum, C.-S., Lan, Z., Funada, R., *et al.*: 'Virtual time-slot allocation scheme for throughput enhancement in a millimeter-wave gbps WPAN cross layer design'. Proc. ICC, Dresden, Germay, June 2009, pp. 1–6
21 Sum, C.-S., Lan, Z., Funada, R., *et al.*: 'Virtual time-slot allocation scheme for throughput enhancement in a millimeter-wave multi-Gbps WPAN system', *IEEE J. Sel. Areas Commun.*, 2009, **27**, (8), pp. 1379–1389
22 Singh, S., Mudumbai, R., Madhow, U.: 'Distributed coordination with deaf neighbors: efficient medium access for 60 GHz mesh networks'. Proc. INFOCOM, San Diego, CA, USA, March 2010, pp. 1–9
23 IEEE standard 802.11ad: '*Standard for Information Technology-Wireless MAN Medium Access Control (MAC) and Physical Layer (PHY) Specifications-Enhancements for Very High Throughput in 60 GHz Band*', 2012
24 Condoluci, M., Dohler, M., Araniti, G., *et al.*: 'Toward 5G densenets architectural advances for effective machine-type communications over femtocells', *IEEE Commun. Mag.*, 2015, **53**, (1), pp. 134–141
25 Tse, D., Viswanath, P.: 'Fundamentals of wireless communication' (Cambridge University Press, 2005)
26 Gross, F.: 'Smart antennas for wireless communications (With MATLAB)' (McGraw-Hill Professional, 2005)
27 Niu, Z.: 'Basic theory of communication networks', Class notes for EE 70230193, Department of Electronic Engineering, Tsinghua University, 2013